Journal of Agricultural Science (2011), **149**, 403–414. © *Cambridge University Press* 2011
doi:10.1017/S0021859610001309

CLIMATE CHANGE AND AGRICULTURE PAPER

Agricultural drought monitoring in semi-arid and arid areas using MODIS data

A. SHAHABFAR* AND J. EITZINGER

Institute of Meteorology (BOKU-Met), Workgroup of Agro-meteorology, Department of Water, Atmosphere and Environment (WAU), University of Natural Resources and Applied Life Sciences (BOKU), Vienna, Peter Jordan Street 82, A-1190 Vienna, Austria

(*Revised MS received 15 September 2010; Accepted 12 October 2010; First published online 18 January 2011*)

SUMMARY

The performances of two remote sensing drought indices were evaluated at selected agricultural sites in different agro-climatic zones in Iran to detect the severity of drought phenomena related to temporal variation and different climatic conditions. The indices used were the perpendicular drought index (PDI) and the modified perpendicular drought index (MPDI), which are derived from moderate resolution imaging spectroradiometer (MODIS) satellite images (MOD13A3 V005). The correlations between these perpendicular indices and two other remote sensing indices in ten different agro-climatic zones of Iran from February 2000 to December 2005 were analysed. The additional indices evaluated were the enhanced vegetation index (EVI) and the vegetation condition index (VCI) along with five water balance parameters, including climatic water balance (CL), crop water balance (CR), monthly reference crop evapotranspiration (ET_0), crop evapotranspiration (ET_c) and required irrigation water (I). Winter wheat was selected as the reference crop because it is grown in the majority of climatic conditions in Iran.

The results show that in several climatic regions, there is a statistically significant correlation between PDI and MPDI and the water balance parameters, indicating an acceptable performance in detecting crop drought stress conditions. In all zones except at the sites located in northwest and northeast of Iran, VCI and EVI are less correlated with the applied water balance indicators compared to PDI and MPDI. In a temporal analysis, PDI and MPDI showed a greater ability to detect CR conditions than VCI and EVI in the most drought-sensitive winter wheat-growing stages. Since Iran is characterized by arid or semi-arid climatic conditions and winter wheat is a major agricultural crop, a combination of both PDI and MPDI could be used as simple remote sensing-based tool to map drought conditions for crops in Iran and in other developing countries with similar climatic conditions.

INTRODUCTION

Drought can have serious impacts on local economies and agricultural production (Ghulam *et al.* 2008). There have been many regional drying trends worldwide over the last three decades (Dai, in press), and many world regions have suffered from water crises (Ghulam *et al.* 2008). Crop water stress is a complex phenomenon that is difficult to detect because crops are able to adjust their physiological status and water consumption by opening and closing stomata. Crop water stress is associated with soil water balance, evaporation, root water uptake and transpiration and other plant biophysical parameters (Yang *et al.* 2008). Therefore, drought-monitoring methods such as satellite remote sensing of surface moisture status and drought conditions are of great interest for sustainable development and management of agricultural production.

Ghulam *et al.* (2007*a*, *b*, 2008) and Qin *et al.* (2008) introduced and developed perpendicular drought indices (PDIs) that were derived from images taken

* To whom all correspondence should be addressed. Email: alireza.shahabfar@boku.ac.at or shahabfar@gmail.com

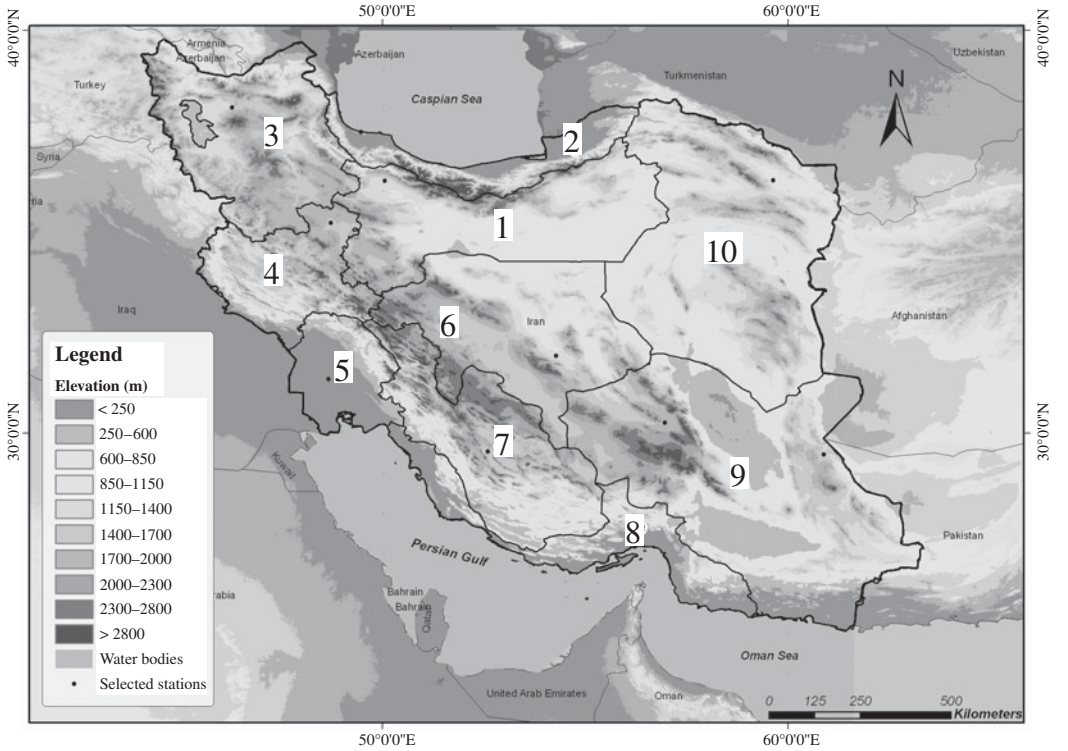

Fig. 1. Geographical locations of agro-ecological zones and selected meteorological stations in Iran – numbers refer to the agro-ecological zones as given in Table 1 (modified from Malakouti *et al.* 2004).

by various satellites over case study locations in China. They found significant relationships between these indices and soil moisture (SM) over different study areas that differed in vegetation coverage from full vegetation cover to bare soil. They recommended applying these methods as drought monitoring indices in semi-arid and arid areas. Shahabfar & Eitzinger (2009) evaluated these perpendicular indices by comparing them with three meteorological drought indices, including Z-score (Z), China-Z index (CZI) and modified China-Z index (MCZI) over different climatic regions in Iran; the analysis included measurements from over 180 weather stations. The results of the present study indicated a strong and significant correlation between the PDI and the three meteorological drought indices. These results also indicated a high, significant correlation between the perpendicular indices and precipitation recorded at the weather stations. The PDI was effective for bare soil applications and in the early stages of vegetation growth, but is not useful for surfaces covered with vegetation. In contrast, the modified PDI (MPDI) showed acceptable performance in vegetated areas.

Iran, situated in western Asia, has an area of more than 1·6 million km^2. The annual precipitation varies from *c.* 25 mm in the Central Plateau to over 2000 mm in the Caspian coastal plain, with a national annual average of 250 mm. Central Iran is a steppe-like plateau with a hot, dry climate (annual rainfall < 200 mm; average summer temperatures > 38 °C) surrounded by desert and mountains (Zagros on the western border and Alborz to the north); *c.* 0·9 of the country is arid or semi-arid (Fig. 1).

Iran has been broadly divided into different agro-ecological zones based on climatic conditions and type of crops grown (Fig. 1 and Table 1). Approximately 0·44 of the cultivated crops in Iran are rain-fed, but they produce only 0·12 of the country's total crop production. However, rain-fed wheat accounts for *c.* 0·35 of the total crop production, and rain-fed barley accounts for *c.* 0·34 of the total production. In comparison, 0·9 of all orchards in Iran are irrigated (Malakouti *et al.* 2004) (Table 2).

Iran frequently experiences recurring droughts. The most recent (1998–2001) was the worst in 30 years, with rainfall deficits consistently falling below 0·6 of the mean annual rainfall in most of the country. The severity of these droughts placed an extreme strain on water resources, livestock and agriculture. Crops from a rain-fed area of 4 million ha and those from an

https://doi.org/10.1017/S0021859610001309 Published online by Cambridge University Press

Table 1. *Description of the agro-ecological zones of Iran (source: Malakouti* et al. *2004) and the selected representative weather stations (weather station data used for calculations of the water balance indicators and surface conditions of 1 km^2 used for the remote sensing drought indices)*

Zone	Agro-ecological zone	Description of zone	Description of selected weather station surroundings	Latitude, longitude and elevation (m asl) of the weather stations and remote sensed area
1	Central	The south-eastern part of the zone is situated in dry climatic conditions, whereas the vast western part has seasonal dry conditions. Majority part of this region covered by winter wheat farms	Within irrigated agricultural farms with semi arid climatologic condition	Lat: 36°15′N Long: 50°3′E m asl: 1279·2
2	Caspian Coastal Plain	Contains wet and humid conditions that cover the coast of the Caspian Sea	Full vegetation coverage, high rainfall, near rain-fed agricultural farms	Lat: 37°28′N Long: 49°28′E m asl: –26·2
3	North-western	This zone covers the north-western part of country. It has seasonal dry periods, moderate summers and extreme winters. Majority of this region is covered by winter wheat farms	Located in mountainous and semi-mountainous region with rain-fed farms	Lat: 38°5′N Long: 46°17′E m asl: 1361·0
4	Central Zagros	With good rainfall in winter, this region is characterized by dry, warm winds in May–June with partial vegetation coverage	Two meteorological stations within rain-fed agricultural farms	Lat: 34°52′N, 34°21′N Long: 48°2′E, 47°9′E m asl: 1741·5, 1318·6
5	Khuzestan	Extremely high transpiration, very hot and humid during summer. During winter, temperatures drop below 0 °C. Full vegetation coverage during the winter time and the majority of winter wheat farms irrigate by permanent rivers that flow in this zone	Contains irrigated agricultural farms surrounded by date palms and Orchards	Lat: 31°20′N Long: 48°40′E m asl: 22·5
6	Arid Central	To the east of this zone is the dry Dasht-e-Kavir desert. Region to the west receives good rainfall	Two meteorological stations located within a semi-arid climatological region with nearby irrigated and rain-fed agricultural farms	Lat: 32°37′N, 31°54′N Long: 51°40′E, 54°17′E m asl: 1550·4, 1237·2
7	Southern Zagros	The average rainfall is above 270 mm. This region is characterized by extremely warm springs with partial vegetation coverage	Irrigated agricultural farms (mostly winter wheat) with high temperature climatological conditions	Lat: 29°32′N Long: 52°36′E m asl: 1484·0
8	Southern Coastal Plain	The average daily temperature rarely drops below 15 °C, and the rate of evapotranspiration is high in winter. This region has seasonal dry conditions with partial vegetation coverage during the rainfall season (monsoon)	A coastal area near irrigated agricultural farms	Lat: 27°13′N Long: 56°22′E m asl: 9·8
9	Arid Southern	With cold winters and warm summers, this zone has similar climatic conditions to zone 8 in that the temperature rarely falls below 15 °C	Two meteorological stations within irrigated agricultural farms (mostly winter wheat)	Lat: 30°15′N, 29°28′N Long: 56°8′E, 60°53′E m asl: 1753·8, 1370·0
10	Khorasan	This zone has an average annual rainfall between 240 and 270 mm. It is characterized by long, cold winters and late rainfall	Near a semi-mountainous area with heterogeneous vegetation and complex rain-fed and irrigated agricultural farms	Lat: 36°16′N Long: 59°38′E m asl: 999·2

Table 2. *Major crop areas of Iran in 2004*

Crop	Area ('000 ha)
Wheat	6600
Barley	1600
Rice	570
Maize	250
Pulses	1185
Oil crops	380
Fruit crops	1141
Vegetable crops	550
Other crops and fallow	4224

Source: Malakouti *et al.* 2004.

irrigated area of 2·7 million ha were completely destroyed during the drought period. By 2001, the total agricultural and livestock losses were estimated as US$2.6 billion. Eighteen out of the country's 28 provinces were affected, but the impact of the drought differed throughout the country (Morid *et al.* 2006).

In view of these problems, the present study re-examines newly developed remote sensing-derived drought indices for applications in the agricultural sector in Iran to contribute for a better preparedness to drought. The focus is on finding relationships between crop water balance (CR) indicators, such as potential and actual evapotranspiration or CR deficits. The main objective is to contribute to the construction of a simple drought-monitoring and crop irrigation decision-making system in Iran that is based on PDI.

MATERIALS AND METHODS

Data sources and preparation

Aiming to construct an agricultural drought-monitoring system for Iran and retest the remote sensing indices over ten agro-climatic zones of Iran, test sites with weather stations were selected. In total, 13 meteorological stations, representing each of the ten agro-climatic zones, were used as shown in Fig. 1. All stations are located within agricultural areas that are far from urban areas and represent the typical agricultural land use of the relevant agro-climatic region including vegetation coverage, crop type, rain-fed or irrigated crops. These stations are used operationally as agro-climatological stations by the Iran Meteorological Organization (IRIMO; Table 1). The data comprised monthly meteorological parameters, mean temperature, maximum temperature, minimum temperature, relative humidity, precipitation, wind speed at a height of 2 m and average daily sunshine from February 2000 to December 2005. The data, obtained from the IRIMO, were quality checked for potential errors (e.g. human or instrumental-based errors) and for data homogeneity. These data were applied to both the climatic water balance (CL) model and the crop water balance model. From Satellite images recorded during the same period by moderate resolution imaging spectroradiometer (MODIS) were applied to derive remote sensing-based drought indices. The indices included in the study are the PDI, the MPDI, the enhanced vegetation index (EVI) and the vegetation condition index (VCI). The Global MOD13A3 (Terra Vegetation Indices Monthly L3 Global 1 km SIN Grid) Version 5 product was used, which is provided monthly at 1 km spatial resolution as a gridded level-3 image in the Sinusoidal projection. This image includes 11 different data sets, which are freely available at the MODIS website in hierarchical data format. In generating these monthly images, the algorithm uses 16 day composite images at 1 km resolution to overlap the months and employ a weighted temporal average for each pixel if data from both periods are cloud free. In the case of clouds within the two 16 day periods, only the maximum reflectance value of each pixel out of the two periods is selected for the monthly image. To assess the advantages and disadvantages of each index in detecting and measuring drought intensity, all calculated indices were compared on the basis of their temporal and spatial extensions.

All of the images were converted to tagged image file format (TIFF), which is applicable for remote sensing and geographic information systems (GIS) software using the MODIS reprojection tool (MRT). By using MRT, four data sets including the EVI, the normalized difference vegetation index (NDVI), the near-infrared (NIR) and red (NIR–Red) reflectance were derived.

Crop-related water balance indicators, including CL, CR, monthly reference crop evapotranspiration (ET_0), crop evapotranspiration (ET_c) and required irrigation water (I), were computed at the weather station sites according to the suggestions of the Food and Agriculture Organization of the United Nations (FAO) for wheat in Iran (Allen *et al.* 1998). The details of this computation are presented below. Pixel values covering an area of about 1 km^2 were used at the weather stations for comparison of the remote sensing indices with the CR indicators. With regard to the test site's description, it was assumed that every pixel represents an overall surface condition of the typical closed cropping areas of the relevant agro-climatic region (Table 1). This is a common method that has been used in other, similar remote sensing studies (Hartmann *et al.* 2003; Ji & Peters 2003; Ghulam *et al.* 2007*a*, *b*, 2008; Qin *et al.* 2008; Jain *et al.* 2009).

Finally, linear regressions were calculated between the applied remote sensing indices (as the drought indicator) and CR indicators in the different

https://doi.org/10.1017/S0021859610001309 Published online by Cambridge University Press

agro-climatic zones using the monthly values. In these calculations, remote sensing data were assumed as independent variables and CR data were assumed as dependent variables. Calculations were performed over several growing seasons at the selected stations from February 2000 to December 2005. The Pearson correlation coefficient (r), has been used previously in similar studies (Lu *et al.* 2007; Yue & Tan 2007), and was used here to compare the relationships of PDI, MPDI, VCI and EVI with CL, CR, ET_0, ET_c and I.

Drought indicators based on CR

The CL model

Several methods and models for assessing CL values have been used by meteorologists and geographers (Wang *et al.* 1998; Zhao *et al.* 2000). The present study applies the following CL model:

$$CL_i = P_i - ET_{0,i} \quad (1)$$

where CL_i is the climatic water balance in month i of the year, P_i represents the precipitation in month i, and ET_0 denotes the monthly ET_0.

Calculations using the Penman–Monteith method, which is recommended by FAO (Allen *et al.* 1998), were based on monthly weather data and the ET_0 in the following form:

$$ET_0 = \frac{0{\cdot}408\Delta(R_n - G) + r(900/(T+273))U_2(e_s - e_a)}{\Delta + r(1 + 0{\cdot}34U_2)} \quad (2)$$

where ET_0 is the reference level of evapotranspiration of a short grass surface without water shortage (mm/day), R_n represents the net radiation at the crop surface (MJ/m^2/day), G denotes the density of soil heat flux (MJ/m^2/day), r is the psychrometric constant (kPa/°C), T is the mean air temperature at a height of 2 m (°C), U_2 represents the wind speed at a height of 2 m (m/s), e_s is the saturation vapour pressure (kPa), e_a denotes the actual vapour pressure (kPa), $e_s - e_a$ represents the saturation vapour pressure deficit (kPa) and Δ denotes the slope of the vapour pressure curve (kPa/°C). Due to a lack of data, the net radiation, R_n, and the density of soil heat flux, G, were estimated using empirical formulas (Allen *et al.* 1998; Yang *et al.* 2008).

The CR model

In the present study, the CROPWAT V4.2 model developed by the Land and Water Development Division of FAO was used to calculate CR parameters (Clarke 1998). The CR is a measure of the difference between the precipitation and the water requirements of crops during crop growth periods. From studies by Zhao (1996), Li *et al.* (2004) and Yang *et al.* (2008), the water balance model can be written as

$$CR_i = P_i - ET_{c,i} \quad (3)$$

where CR_i is the crop water balance in month i (mm), P_i represents the precipitation during month i (mm) and ET_c is the monthly crop reference evapotranspiration (mm).

ET_c is the amount of water used by a specific crop without water shortage and can be calculated using the crop coefficient approach (Allen *et al.* 1998; Fan & Cai 2002). This approach can be written as

$$ET_c = K_c \times ET_0 \quad (4)$$

where K_c is a crop-related coefficient (Yang *et al.* 2008). Winter wheat, being one of the most important agricultural crops in Iran and able to grow in all of the country's different climatic regions, was selected as a reference in the present study. In general, the growing period of winter wheat starts in late October and lasts until July (Ziaei & Sepaskhah 2003). The K_c was simulated by the CROPWAT model and varies depending on the developmental stage (Allen *et al.* 1998).

The I/crop water deficit

The I accounts for the difference between the effective precipitation and the water requirements of crops during crop growth periods; therefore, it also represents the crop water deficit. The following equation was used to calculate this parameter:

$$I_i = Re_i - ET_{c,i} \quad (5)$$

where I_i is the required irrigation water or crop water deficit in month i (mm) and Re_i represents the effective precipitation during month i (mm), which is related to the mean monthly precipitation and the mean monthly consumptive water use considering soil and crop type (Dastane 1978). The soil-type data from the Land and Water Development Division of FAO were used (Land and Water Development Division 2003).

Remote sensing-based drought indices

PDI – background

Vermote *et al.* (1997) and Ghulam *et al.* (2007*a*) found that in a scatter plot of the atmospheric corrected near-infra-red (NIR) and red (NIR–Red) reflectance spectrum of any satellite image, a typical triangle shape is evident that reflects vegetation and SM conditions (Fig. 2). In Fig. 2, the AD line represents the change of surface vegetation from full cover (A) and partial cover (E) to bare soil (D). In contrast, BC refers to the SM status of the wet area (B) to the semi-arid surface and the extremely dry surface (C). As demonstrated, BC shows the direction of drought severity. Close but complex relationships exist between the surface spectrum, land cover types and

https://doi.org/10.1017/S0021859610001309 Published online by Cambridge University Press

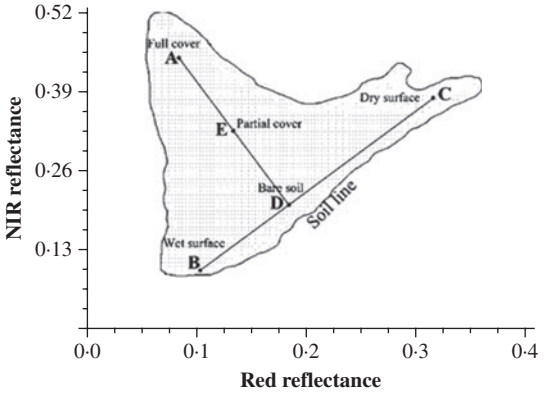

Fig. 2. A typical triangle shape on NIR–Red spectral space (source: Ghulam *et al.* 2007*a*).

surface drought conditions. In addition, different land cover types manifest a certain regular distribution in the NIR–Red spectral space. From this information, the vegetation coverage can be described and the surface drought severity can be characterized quantitatively in the space. Ghulam *et al.* (2007*a*) proposed the construction of an orthogonal axes system above the previously mentioned triangular shape (Fig. 3) and presented two perpendicular remote sensing-based drought indices from this orthogonal axes system.

PDI

The mathematical formula for PDI can be written as follows:

$$\mathrm{PDI} = \frac{1}{\sqrt{M^2+1}}(R_{\mathrm{Red}} + MR_{\mathrm{NIR}}) \qquad (6)$$

where R_{NIR} and R_{Red} are the atmospherically corrected surface reflectances of NIR–Red and NIR bands of remotely sensed data, and M represents the slope of the soil line in the NIR–Red feature space (Ghulam *et al.* 2007*a*). The PDI is a line segment parallel to the soil line and perpendicular to the normal of the soil line that dissects the coordinate origin. The PDI describes the distribution of SM in the NIR–Red feature space. Points far from the normal line in the NIR–Red space correspond to surfaces with a low SM, whereas points near the normal line represent wet surfaces. The PDI, based on the NIR–Red spectral space, is simple and easy to obtain. The PDI values vary between 0 and 1. A large PDI indicates severe water stress, whereas small PDI indicates low water stress. Since many soil biophysical features, including soil surface colour and vegetation conditions, affect NIR and NIR–Red reflectance, this index requires a local calibration to obtain the coefficient M over the different study areas or sample windows.

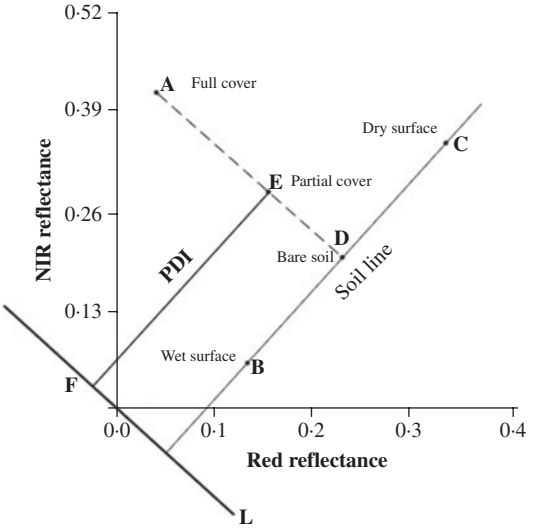

Fig. 3. Construction of an orthogonal axes system on NIR–Red spectral space (source: Ghulam *et al.* 2007*a*).

The PDI is effective for bare soil applications. However, there are some limitations that challenge the performance of the PDI in areas where the surface cover types vary from bare soil to densely vegetated surfaces and are characterized by non-flat topography with different soil types (Ghulam *et al.* 2007*b*).

MPDI

According to the definition of the PDI, areas with full vegetation cover, partial cover and dry bare soil may have the same perpendicular distance from a reference line and, therefore, have the same PDI value. The maximum PDI value, which is expected over dry bare soil, might also be observed over a vegetated surface. As a consequence, the PDI indicates 'drought' for agricultural lands when the corresponding bare soil is defined as stressed, even if there is no drought. Ghulam *et al.* (2007*b*) introduced the term f_{v} into the PDI to separate the effects of vegetation on the index and called it the MPDI, expressed as

$$\mathrm{MPDI} = \frac{R_{\mathrm{Red}} + MR_{\mathrm{NIR}} - f_{\mathrm{v}}\left(R_{\mathrm{v,Red}} + MR_{\mathrm{v,NIR}}\right)}{\left(1-f_{\mathrm{v}}\right)\sqrt{M^2+1}} \qquad (7)$$

where f_{v} is the fraction of vegetation defined as the fraction of ground surface covered by vegetation (Baret *et al.* 1995), $R_{\mathrm{v,Red}}$ and $R_{\mathrm{v,NIR}}$ are the pure vegetation reflectances in the NIR–Red and NIR bands, respectively, and may be regarded as coefficients. When leaf water content, leaf angle distribution, sun and viewing geometry are assumed to be fixed, variations in canopy reflectance are dependent on f_{v} (i.e. it is f_{v}, not $R_{\mathrm{v,Red}}$ and $R_{\mathrm{v,NIR}}$, that causes the

https://doi.org/10.1017/S0021859610001309 Published online by Cambridge University Press

Table 3. *Significant correlations between the monthly drought indices and crop-related water balance indicators for the different agro-ecological zones of Iran from February 2000 to December 2005 (from highest to lowest; numbers refer to the agro-ecological zones as given in Table 1 – only regions with significant correlations are shown)*

	PDI High>>low	MPDI High>>low	VCI High>>low	EVI High>>low
ET_0	5>4>1>2>6>3>9>7>8>10*	5>1>2>4>6>9>7>8>3	3>10>1>2>5>8	2>1>3>10>4>7>8
ET_c	5>4>1>2>8>6>9>3>7	5>1>4>2>6>9>8>7>3*	3>10>5>1>2>8	2>3>10>4>7*>8*
I	5>4>1>2>8>6>9>3>7	5>1>4>6>2>9>8>7>3	3>10>5>2>1>8	3>2>1>10>4*>7*>8*
CL	5>4>1>2>6>7>3>9>8>10*	5>1>4>6>2>7>9>8>3	3>10>1>5>8>2	3>1>10>2>7>4>8*>5*
CR	5>4>1>2>7>8>6>3>9	5>1>4>6>2>7>9>8>3	3>10>5>1>8>2*	3>1>10>2>7>4>8*
	Range of the correlations (maximum–minimum, related to the ranking above)			
ET_0	0·85–0·28*	0·87–0·34	0·76–0·42	0·78–0·31
ET_c	0·81–0·23	0·81–0·31*	0·51–0·42	0·71–0·26*
I	0·82–0·46	0·82–0·32	0·66–0·43	0·68–0·27*
CL	0·86–0·26*	0·88–0·35	0·76–0·39	0·74–0·27*
CR	0·84–0·41	0·85–0·34	0·66–0·31*	0·69–0·26*

* Correlation in this zone is significant at $P<0·05$ (2-tailed); others are significant at $P<0·01$ (2-tailed).

canopy reflectance variations). In the present study, $R_{v,Red}$ and $R_{v,NIR}$ have estimated values of 0·05 and 0·5, respectively (Ghulam *et al.* 2007*b*). Similar to the PDI, the MPDI is derived using the NIR–Red and NIR reflectances, but it is dependent on the SM status and on vegetation growth, which is characterized by activity rates, greenness and stress levels.

EVI

The EVI was developed by Huete *et al.* (2002) for use with MODIS data. Unlike NDVI, it takes advantage of multiple bands. The EVI is calculated as follows:

$$\mathrm{EVI} = G_a \times \frac{R_{NIR} - R_{Red}}{R_{NIR} - C_1 R_{Red} - C_2 R_{Blue} + L} \qquad (8)$$

where R_{Blue} is the blue band reflectance, C_1 and C_2 are the atmosphere resistance red and blue correction coefficients, respectively, L is the canopy background brightness correction factor and G_a is the gain factor.

VCI

This index was first described by Kogan (1995, 1997). It effectively shows how close the current month's NDVI is to the minimum NDVI, as calculated from the long-term record of remote sensing images. This index is calculated as follows:

$$\mathrm{VCI}_i = \left(\frac{\mathrm{NDVI}_i - \mathrm{NDVI}_{min}}{\mathrm{NDVI}_{max} - \mathrm{NDVI}_{min}}\right) \times 100 \qquad (9)$$

where NDVI_{max} and NDVI_{min} are calculated from the long-term record (20 years) for that month (or week), and i is the index of the current month (or week). The condition (health) of the vegetation, represented by the VCI, is reported as a proportion and may serve as an approximate measure of the dryness of the current month. During extremely dry months, the vegetation conditions are poor and the VCI is close to or equal to zero. A VCI of 0·5 reflects fair vegetation conditions. At optimal vegetation conditions, the VCI is close to 1·0. At this condition, NDVI for the current time step (month, week) is equal to NDVI_{max}.

RESULTS

The results of the present study are presented in two parts: spatial and temporal analyses.

Spatial analysis of remote sensing indices

The spatial comparison between the test sites of the relevant agro-climatic zones is based on the monthly drought indicators from 2007 to 2009 (3 years). The results indicate that there are different relationships between the remote sensing indices PDI, MPDI, VCI and EVI *v.* the different CR indices, depending on location and the relevant agro-climatic zone (Table 3).

https://doi.org/10.1017/S0021859610001309 Published online by Cambridge University Press

In zone 1, which is characterized by dry climatic conditions (Table 1), the test site is covered by irrigated crop fields, and MPDI performs better than PDI, VCI and EVI. For example, the correlation between MPDI and I is 0·68 ($P<0·01$), but for PDI, VCI and EVI this correlation is 0·63, 0·45 and 0·63 ($P<0·01$, data not shown). This zone includes the largest irrigated area, reflecting the lack of precipitation during the growing season, and the fact that the majority of the zone is covered by agricultural fields. MPDI showed the highest correlation with the crop water deficit indicator I in zone 1.

In zone 2, the test site with full vegetation coverage, the remote sensing indices behave very similar to those in zone 1. This zone is characterized by wet and humid conditions, and the majority of this zone, including the test site, is dominated by rain-fed cropping.

In zone 3, which covers a large part of the high mountainous area of Iran, VCI and EVI perform better than PDI and MPDI. Under these agro-climatic conditions, EVI and VCI perform well for detecting CR conditions. Similar results have been demonstrated previously (Shahabfar & Eitzinger 2009).

Zone 4 is located in the semi-mountainous area of Iran. According to the present results at this station, PDI has the highest correlation with ET_0 ($r=0·73$), ET_c ($r=0·65$), I ($r=0·64$), CL ($r=0·74$) and CR ($r=0·68$) (all $P<0·01$) and MPDI perform better than the other remote sensing indices VCI and EVI (not statistically significant).

The test site in zone 5 is located within densely irrigated farms in Khuzestan province. Extreme transpiration and very hot and humid conditions are the main climatic characteristics of this zone (Table 1). This zone also belongs to the most productive agricultural region in Iran. The main crop is winter wheat, which grows during the cold season. During the warm season, dates and orchard fruits are produced. Here, MPDI and PDI show the highest correlations with CR parameters (Table 3). For example, the highest correlations between PDI and MPDI *v.* ET_0 are 0·85 and 0·87, respectively (for both correlations $P<0·01$).

The test sites in zones 6–9 represent arid or semi-arid regions of Iran, where the major climatic characteristics are low precipitation and humidity, and hot, dry seasons. The major agricultural crop in these zones is irrigated winter wheat. Ground water and seasonal rivers that flow during rainfall seasons are the main irrigation resources in these semi-arid to arid regions. In these zones, the correlation between the MPDI and ET_0, ET_c, I, CL and CR is stronger than those of the other remote sensing indices including PDI, VCI and EVI.

The selected weather station in zone 10 is located in a semi-mountainous area surrounded by different vegetation types including complex rain-fed and irrigated farms. At the study site of this zone, VCI showed the best correlation to the water balance indicators, similar to zone 3 (Table 3).

Temporal analysis of remote sensing indices

Figure 4 shows monthly comparisons of several indices in two different agro-climatological zones, 1 and 10, which are the two regions with the best and worst results. The study period from February 2000 to December 2005, includes five separate growing seasons. For comparison, all indices were standardized (index values minus the average of the index during the study period divided by standard deviation). Figure 4*a* indicates that in several winter wheat-growing periods, there is a strong relationship between the PDI and MPDI and the applied CR parameters. With the exception of zones 3, 4 and 10, during the first three growing seasons of 2000/01, 2001/02 and 2002/03, there were significant correlations between fluctuations in the PDI and MPDI and the CR indicators. Therefore, the PDI and MPDI were able to reflect drought conditions but were subject to variation in different years, showing a higher temporal relationship with all of the five studied CR parameters compared to the other remote sensing indices, especially in periods of wheat development (Table 4) from February 2000 to December 2005.

DISCUSSION

A good agricultural drought monitoring system should be able to account for the variable susceptibility of crops during different stages of crop development, focusing on precipitation shortages, differences between actual and potential evapotranspiration and soil water deficits (Rhee *et al.* 2010). Therefore, the present study evaluated several drought indices for Iran, focusing on MPDI and PDI and other remote sensing based indices to detect the severity of drought phenomena for agricultural crop production. Both the temporal and spatial variations were evaluated and compared with CR indicators at selected agricultural sites in different agro-climatic zones.

In a previous study by Shahabfar & Eitzinger (2009), PDI and MPDI were compared with meteorological drought indices at 180 meteorological stations over Iran. Those authors also found that in the northern region of zone 10, where the vegetation coverage varies from dense to average, MPDI performed best for drought detection. In comparison, in the middle and southern region, which has poor vegetation coverage or bare soil, PDI showed the best relative performance.

There are several previous studies where indices such as NDVI, VCI and EVI were used for vegetation condition monitoring in arid and semi-arid regions

https://doi.org/10.1017/S0021859610001309 Published online by Cambridge University Press

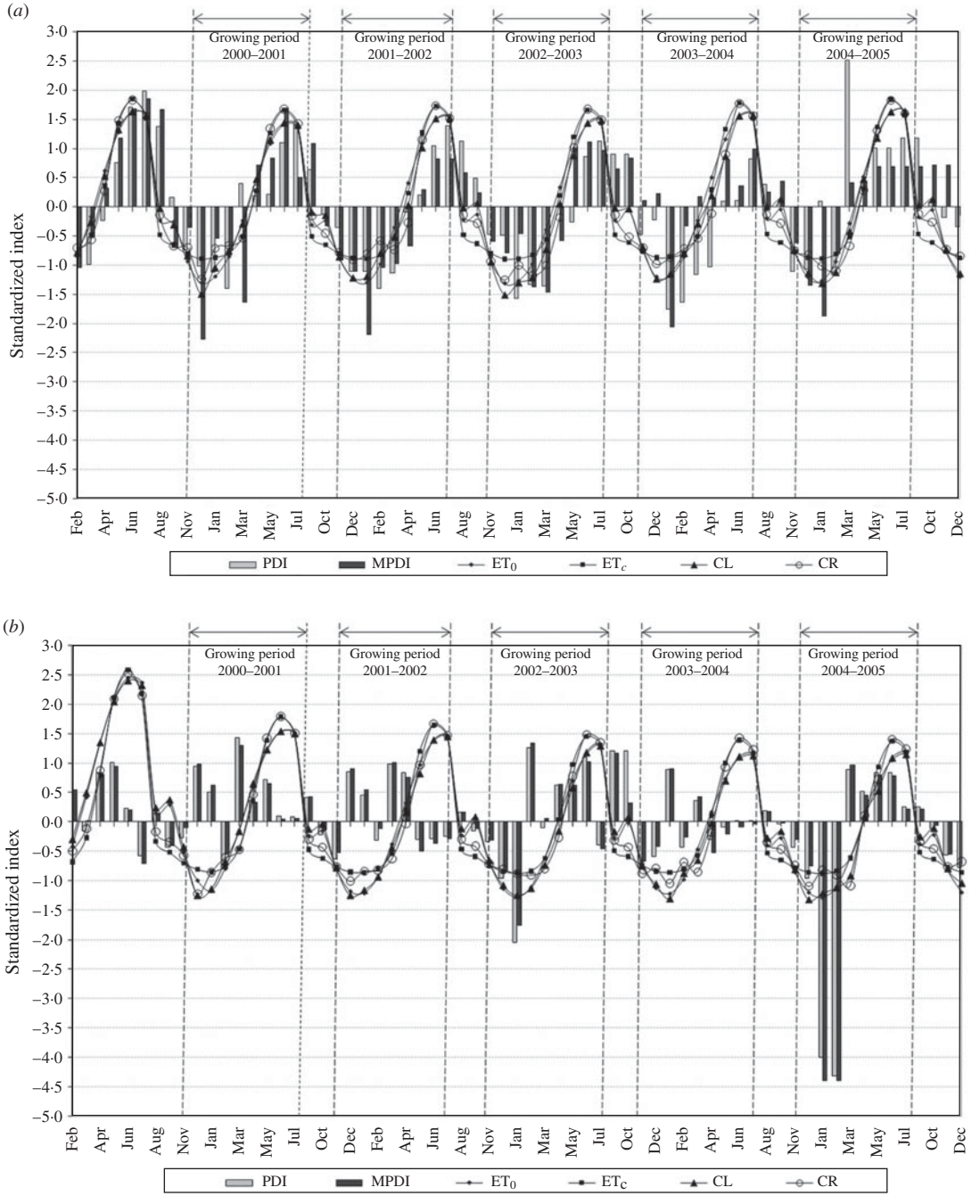

Fig. 4. The temporal distribution of remote sensing indices *v*. crop water parameters for the period from February 2000 to December 2005 in two agro-climatological zones of Iran: (*a*) zone 1 and (*b*) zone 10.

(Diouf & Lambin 2001; Singh *et al*. 2003; Song *et al*. 2004; Sun *et al*. 2004; Anyamba & Tucker 2005; Bhuiyana *et al*. 2006; Martiny *et al*. 2006; Bajgiran *et al*. 2008; Murthy *et al*. 2009; Quiring & Ganesh 2010). All of these studies concluded that NDVI, VCI and EVI could be used as indicators in drought early warning systems based on the received correlations between precipitation and/or biomass.

https://doi.org/10.1017/S0021859610001309 Published online by Cambridge University Press

Table 4. *Significant correlations between drought indices and crop-related water balance indicators over Iran for the different months (from highest to lowest; numbers refer to months, starting with January = 1 and ending with December = 12 – only months with significant correlations are shown)*

	PDI High > > low	MPDI High > > low	VCI High > > low	EVI High > > low
ET_0	4 > 12 > 5 > 2 > 11 > 10 > 6 > 3 > 7 > 8 > 1	2 > 4 > 5	7 > 6 > 10 > 8 > 11 > 5 > 4 > 12 > 3 > 1*	6 > 7 > 8 > 10 > 5 > 4 > 11*
ET_c	4 > 12 > 5 > 2 > 11 > 10 > 6 > 3 > 7 > 8 > 1	2 > 4 > 5*	7 > 6 > 10 > 8 > 11 > 5 > 4 > 12 > 3 > 2*	6 > 7 > 8 > 10 > 5 > 4 > 11*
I	4 > 5 > 11 > 6 > 8 > 10 > 7 > 12 > 3 > 2 > 1*	1 > 4 > 2 > 5* > 12*	7 > 6 > 10 > 8 > 11 > 5 > 4 > 12 > 3 > 1 > 2	6 > 7 > 10 > 5 > 8 > 4 > 11* > 3*
CL	4 > 5 > 12 > 11 > 2 > 6 > 10 > 3 > 8 > 7 > 1	4 > 2* > 5* > 1*	7 > 6 > 8 > 5 > 10 > 11 > 4 > 12 > 3 > 1 > 2	6 > 7 > 8 > 5 > 4 > 10*
CR	4 > 5 > 6 > 11 > 7 > 8 > 10 > 12 > 3 > 2 > 1	4 > 5* > 1*	6 > 7 > 5 > 8 > 4 > 11 > 10 > 3 > 1 > 12 > 2*	6 > 7 > 5 > 4 > 8*
	Range of the correlation (maximum–minimum, related to the ranking above)			
ET_0	0·80–0·34	0·30–0·26	0·71–0·22*	0·57–0·25*
ET_c	0·80–0·34	0·30–0·26*	0·71–0·28*	0·57–0·25*
I	0·83–0·31*	0·46–0·22*	0·69–0·32	0·54–0·22*
CL	0·83–0·40	0·31–0·26*	0·70–0·31	0·55–0·26*
CR	0·82–0·34	0·32–0·26*	0·68–0·26*	0·53–0·26*

* Correlation in this zone is significant at $P < 0{\cdot}05$ (2-tailed); others are significant at $P < 0{\cdot}01$ (2-tailed).

For example, Diouf & Lambin (2001) found that over the test sites in Ferlo, Senegal, the mean correlation between NDVI and biomass during 1988–1995 was 0·68 ($P < 0{\cdot}01$). Anyamba & Tucker (2005) found that the correlation between NDVI and rainfall anomaly time series for 1981–2000 was positive and significant at 0·78 in the Sahel region. Sun *et al.* (2004) concluded that annual evapotranspiration is highly correlated with integrated NDVI with a correlation coefficient of 0·77. These results were obtained from recorded data in meteorological stations located in the Yellow River Basin, China, in 1992. According to Quiring & Ganesh (2010), the mean relationship between VCI and meteorological drought indices including Zscore, Palmer Drought Index, Standardized Precipitation Index (1-, 2-, 3-, 6-, 9-, 12- and 24-month), proportion of normal and deciles based in 254 Texas counties are 0·33, 0·51 ($P < 0{\cdot}05$), 0·20, 0·38, 0·44, 0·53 ($P < 0{\cdot}05$), 0·51 ($P < 0{\cdot}05$), 0·44, 0·34, 0·17 and 0·20, respectively.

In the present study, the VCI and EVI in all zones are less correlated with the applied water balance indicators compared to PDI and MPDI, except at the sites in zones 3 (northwest of Iran) and 10 (northeast of Iran). Bajgiran *et al.* (2008) also found that in the northwest of Iran VCI (and NDVI) showed a strong correlation with average 3-month precipitation. They concluded that both VCI and NDVI show good performance in monitoring of vegetation condition in this area and suggested VCI as drought index in this area at regional scale. However, they recommended that for obtaining more reliable results their approach must be tested in different climates, using a combination of different climatic factors (such as temperature and precipitation). The present study confirms that at the test sites covered with complex and heterogeneous vegetation types, neither the MPDI nor the PDI perform satisfactorily. Their performances could be improved, however, with increased spatial resolution of the applied satellite images.

As shown by the results of the temporal analysis, the correlations between the remote sensing drought indices and crop-related water balance indicators vary by month. The MPDI shows the best results in April during the heading and flowering stages of winter wheat. In contrast, the PDI show the best results during January, February and April during the jointing stage of winter wheat with less vegetation coverage. Therefore, both PDI and MPDI in combination show the best performance during the full winter wheat-growing season, where this crop is very sensitive to drought. Referring to Eqn (6), PDI is a function of infrared (IR), NIR and the slope of the soil line in the NIR–Red feature space (M), and unlike MPDI does not contain a vegetation component. Therefore, this perpendicular index is a good indicator of SM for bare soil or partially uncovered soil. However, the VCI and EVI performed better than

https://doi.org/10.1017/S0021859610001309 Published online by Cambridge University Press

the perpendicular indices in June and July. These months represent the final growing stage of winter wheat when the use of drought monitoring or water management is less beneficial.

Overall, the spatial analysis results show that the strongest correlation between the studied remote sensing indices and crop-related water balance indicators belongs to PDI in regions or sites with homogeneous vegetation, which was the case in eight out of ten agro-ecological zones in Iran. The temporal analysis shows that PDI performs best at the early growing stages and MPDI is better for full vegetation coverage or late crop development stages. In contrast, the remote sensing indices VCI and EVI performed better in heterogeneous vegetated areas or very late crop development stages of wheat. The present study confirms the results presented by Ghulam *et al*. (2007*a*, *b*, 2008) and Qin *et al*. (2008). Because of the semi-arid and arid conditions found throughout Iran and considering that winter wheat is a major agricultural crop in Iran, PDI (for partly covered vegetated areas) and MPDI (for fully covered vegetated areas) can be used as simple and cost-efficient drought indices derived from MODIS satellite images. This finding has potential significance for agricultural crop growing regions in other developing countries with similar climatic conditions. To further improve the accuracy of the achieved results and reduce the level of uncertainties, the use of additional field observations, more ground-based soil water content measurements, considering other important crops or crop rotations and increasing the temporal resolution of remote sensing indices (weekly or daily images) is recommended.

This work was supported by the Austrian Agency for International Cooperation in Education and Research (OeAD). The authors would like to thank Dr. Abuduwasiti Wulamu for his constructive comments. They would also like to thank the Iran Meteorological Organization (IRIMO), which provided the meteorological data required for this study, and the US Geological Survey (USGS) Earth Resources Observation and Science (EROS) Center, which provided the MODIS satellite images that were used in this paper. The authors would like to extend their thanks to the anonymous reviewers for their valuable comments and suggestions.

REFERENCES

Allen, R. G., Pereira, L. S., Raes, D. & Smith, M. (1998). *Crop Evapotranspiration Guidelines for Computing Crop Water Requirements*. FAO Irrigation and Drainage Paper No. 56. Rome, Italy: FAO.

Anyamba, A. & Tucker, C. J. (2005). Analysis of Sahelian vegetation dynamics using NOAA-AVHRR NDVI data from 1981–2003. *Journal of Arid Environments* **63**, 596–614.

Bajgiran, P. R., Darvishsefat, A. A., Khalili, A. & Makhdoum, M. F. (2008). Using AVHRR-based vegetation indices for drought monitoring in the Northwest of Iran. *Journal of Arid Environments* **72**, 1086–1096.

Baret, F., Clevers, J. G. P. W. & Steven, M. D. (1995). The robustness of canopy gap fraction estimates from red and near-infrared reflectances: a comparison of approaches. *Remote Sensing of Environment* **54**, 141–151.

Bhuiyana, C., Singha, R. P. & Kogan, F. N. (2006). Monitoring drought dynamics in the Aravalli region (India) using different indices based on ground and remote sensing data. *International Journal of Applied Earth Observation and Geoinformation* **8**, 289–302.

Clarke, D. (1998). *CROPWAT for Windows User's Guide*, version 4.2. Southampton, UK: Institute of Irrigation and Development Studies (IIDS), University of Southampton.

Dai, A. (in press). Drought under global warming: a review. *Wiley Interdisciplinary Reviews: Climate Change*. doi: 10.1002/wcc.81.

Dastane, N. G. (1978). *Effective Rainfall in Irrigated Agriculture*. FAO Irrigation and Drainage Papers 25. Rome, Italy: FAO.

Diouf, A. & Lambin, E. F. (2001). Monitoring land-cover changes in semi-arid regions: remote sensing data and field observations in the Ferlo, Senegal. *Journal of Arid Environments* **48**, 129–148.

Fan, Y. Q. & Cai, H. J. (2002). Comparison of crop water requirements computed by single crop coefficient approach and dual crop coefficient approach. *Journal of Hydraulic Engineering* **3**, 50–54.

Ghulam, A., Qin, Q., Kusky, T. & Li, Z. L. (2008). A re-examination of perpendicular drought indices. *International Journal of Remote Sensing* **29**, 6037–6044.

Ghulam, A., Qin, Q., Teyip, T. & Li, Z. L. (2007*b*). Modified perpendicular drought index (MPDI): a real-time drought monitoring method. *ISPRS Journal of Photogrammetry and Remote Sensing* **62**, 150–164.

Ghulam, A., Qin, Q. & Zhan, Z. (2007*a*). Designing of the perpendicular drought index. *Environmental Geology* **52**, 1045–1052.

Hartmann, T., di Bella, C. & Oricchio, P. (2003). Assessment of the possible drought impact on farm production in the SE of the province of Buenos Aires, Argentina. *ISPRS Journal of Photogrammetry and Remote Sensing* **57**, 281–288.

Huete, A., Didan, K., Miura, T., Rodriguez, E. P., Gao, X. & Ferreira, L. G. (2002). Overview of the radiometric and biophysical performance of the MODIS vegetation indices. *Remote Sensing of Environment* **83**, 195–213.

Jain, S. K., Keshri, R., Goswami, A., Sarkar, A. & Chaudhry, A. (2009). Identification of drought-vulnerable areas using NOAA AVHRR data. *International Journal of Remote Sensing* **30**, 2653–2668.

Ji, L. & Peters, A. J. (2003). Assessing vegetation response to drought in the northern Great Plains using vegetation and drought indices. *Remote Sensing of Environment* **87**, 85–98.

Kogan, F. N. (1995). Application of vegetation index and brightness temperature for drought detection. *Advances in Space Research* **15**, 91–100.

Kogan, F. N. (1997). Global drought watch from space. *Bulletin of the American Meteorological Society* **78**, 621–636.

Land and Water Development Division (2003). *Digital Soil Map of the World and Derived Soil Properties* (On CD-ROM). Rome, Italy: FAO.

Li, Y. L., Gao, S. H. & Gua, J. P. (2004). Analysis of water supply and demand for crops in the dry cropland of China. *Climatic and Environmental Research* **9**, 331–341 (in Chinese).

Lu, Y., Tao, H. & Wu, H. (2007). Dynamic drought monitoring in Guangxi using revised temperature vegetation dryness index. *Wuhan University Journal of Natural Sciences* **12**, 663–668.

Malakouti, M. J., Khoughar, Z. & Khademi, Z. (2004). *Innovative Approaches to Balanced Nutrition of Wheat: a Compilation of Papers*. Agronomy Department. Ministry of Jihad-e-Agriculture. Tehran, Iran: Sana Publishing Co.

Martiny, N., Camberlin, P., Richard, Y. & Philippon, N. (2006). Compared regimes of NDVI and rainfall in semi-arid regions of Africa. *International Journal of Remote Sensing* **27**, 5201–5223.

Morid, S., Smakhtin, V. & Moghaddasi, M. (2006). Comparison of seven meteorological indices for drought monitoring in Iran. *International Journal of Climatology* **26**, 971–985.

Murthy, C. S., Sesha Sai, M. V. R., Chandrasekar, K. & Roy, P. S. (2009). Spatial and temporal responses of different crop-growing environments to agricultural drought: a study in Haryana state, India using NOAA AVHRR data. *International Journal of Remote Sensing* **30**, 2897–2914.

Qin, Q., Ghulam, A., Zhu, L., Wang, L., Li, J. & Nan, P. (2008). Evaluation of MODIS derived perpendicular drought index for estimation of surface dryness over northwestern China. *International Journal of Remote Sensing* **29**, 1983–1995.

Quiring, S. M. & Ganesh, S. (2010). Evaluating the utility of the Vegetation Condition Index (VCI) for monitoring meteorological drought in Texas. *Agricultural and Forest Meteorology* **150**, 330–339.

Rhee, J., Im, J. & Carbone, G. J. (2010). Monitoring agricultural drought for arid and humid regions using multi-sensor remote sensing data. *Remote Sensing of Environment* **114**, 2875–2887.

Shahabfar, A. & Eitzinger, J. (2009). Different responses of MODIS-derived drought indices in a variety of agro-climatic conditions. In *Impact of Climate Change and Adaptation in Agriculture. International Symposium, University of Natural Resources and Applied Life Sciences (BOKU), Vienna, 22–23 June 2009. Extended Abstracts* (Eds J. Eitzinger & G. Kubu), pp. 140–143. BOKU-Met Report 17. Vienna: BOKU. Available online at: http://www.adagio-eu.org/documents/BOKU_Met_Report_17.pdf (Verified 17 Nov 2010).

Singh, R. P., Roy, S. & Kogan, F. (2003). Vegetation and temperature condition indices from NOAA AVHRR data for drought monitoring over India. *International Journal of Remote Sensing* **24**, 4393–4402.

Song, X., Saito, G., Kodama, M. & Sawada, H. (2004). Early detection system of drought in East Asia using NDVI from NOAA/AVHRR data. *International Journal of Remote Sensing* **25**, 3105–3111.

Sun, R., Gao, X., Liu, C. M. & Li, X. W. (2004). Evapotranspiration estimation in the Yellow River Basin, China using integrated NDVI data. *International Journal of Remote Sensing* **25**, 2523–2534.

Vermote, F. E., Tanre, D., Deuze, L. J., Herman, M. & Morcrette, J. J. (1997). Second simulation of the satellite signal in the solar spectrum: an overview. *IEEE Transactions on Geoscience and Remote Sensing* **35**, 675–686.

Wang, D. W., Zhou, D. M., Zhang, J. P. & Zang, S. G. (1998). Research on soil moisture dynamics and production effect of water-fertilized coupling in the dry land of Taihanshan Mountain area. *Agricultural Research in Arid Areas* **16**, 32–40 (in Chinese).

Yang, Y., Fenga, Z., Huang, H. Q. & Lin, Y. (2008). Climate-induced changes in crop water balance during 1960–2001 in Northwest China. *Agriculture, Ecosystems and Environment* **127**, 107–118.

Yue, W. & Tan, W. (2007). The relationship between land surface temperature and NDVI with remote sensing: application to Shanghai Landsat 7 ETM+ data. *International Journal of Remote Sensing* **28**, 3205–3226.

Zhao, J. B., Xu, Z. L., Zhong, Z. Z. & Mao, X. S. (2000). *Field Water Balance in the Dry Land of Northwest China*. Beijing: China Agriculture Press (in Chinese).

Zhao, S. L. (1996). *Introduction to Catchment Agriculture*. Xi'an, China: Shaanxi Science and Technology Press (in Chinese).

Ziaei, A. N. & Sepaskhah, A. R. (2003). Model for simulation of winter wheat yield under dryland and irrigated conditions. *Agricultural Water Management* **58**, 1–17.